

Buffer-gas loaded magneto-optical traps for Yb, Tm, Er and Ho

Boerge Hemmerling,^{1,2,*} Garrett K. Drayna,^{1,2,3} Eunmi Chae,^{1,2} Aakash Ravi,^{1,2} and John M. Doyle^{1,2}

¹Harvard-MIT Center for Ultracold Atoms, Cambridge, Massachusetts 02138, USA

²Department of Physics, Harvard University, Cambridge, Massachusetts 02138, USA

³Department of Chemistry, Harvard University, Cambridge, Massachusetts 02138, MA

Direct loading of magneto-optical traps from a very slow cryogenic buffer-gas beam of lanthanides is achieved and studied, without the need for laser slowing. A collisionally cooled cryogenic atomic source with average forward velocity of 60-70 m/s and a width of ~ 70 m/s allows for loading without additional dissipation, unlike oven or supersonic sources. The lanthanides Yb, Tm, Er, and Ho are trapped. Despite the He buffer-gas background, we observe a maximum lifetime of about 80 ms (with Yb). We further show that the addition of a single-frequency slowing laser increases the number of trapped Yb atoms by an order of magnitude, yielding a total of $4.0(2) \times 10^8$. We study decay to metastable states in all species and report decay rates. Extension of this approach to MOTs of molecules is discussed.

The invention of laser and evaporative cooling of atoms has led to significant new discoveries: frequency standards and precision spectroscopy [1], quantum computation [2, 3], studies of cold collisions [4] and degenerate quantum gases [5]. Initially, laser cooling experiments were thought to be restricted to "closed cycle" species, those which do not show spontaneous decay into metastable states. Such processes remove the atom from the cooling cycle. For this reason, the first laser cooling experiments were carried out with alkali and alkaline-earth atoms. In later experiments, more complex species were cooled and trapped, even those with so-called optical "leaks". Notable examples include Yb [6], Cr [7, 8], Tm [9], Er [10, 11] and Dy [12], with the latter four being of recent high interest, due to their highly magnetic ground states. In contrast to alkali atoms, which mainly experience a short-range contact potential caused by the van der Waals force, the large magnetic dipole moments of Tm ($4 \mu_B$), Er ($7 \mu_B$), Cr ($6 \mu_B$) and Dy ($10 \mu_B$) allow for the study of systems with long-range dipole-dipole interactions [13] and the testing of fundamental theories [12]. More generally, ultracold non S -state atoms can be used for studies of exotic quantum phases and quantum magnetism [14].

Most recently, there has been renewed interest in moving atom cooling technologies into the realm of molecules. The additional degrees of freedom in molecules are predicted to lead to novel studies. Ultracold diatomic polar molecules are proposed candidates for novel quantum information and simulation experiments [15, 16] and ultracold chemistry studies [17, 18]. But the kind of molecule necessary for a particular study depends strongly on the desired physics. A method to provide a high phase-space density of a variety of molecules in the mK regime is required, but is unavailable at present. One particular class of molecules that may be amenable to 3-D MOT trapping is that with highly diagonal Frank-Condon factors. Recent experiments employing hydrodynamically enhanced buffer-gas beam sources [19] have reported the slowing and cooling of SrF [20, 21] and the creation of a two-dimensional magneto-optical trap for YO [22], and thus successfully showed that even molecules can be laser cooled to a certain extent. Work is ongoing in several groups to create 3-D MOTs for these molecules. Furthermore, laser cooling of

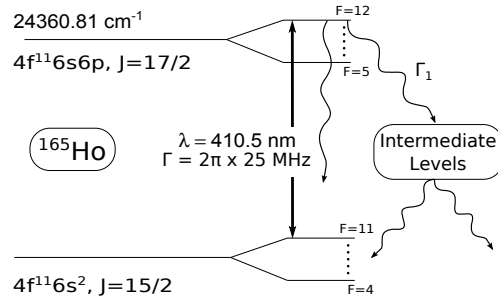


FIG. 1. Partial level scheme of ^{165}Ho with the laser cooling transition. Only the decay to metastable states (Γ_1) is considered for modeling the detuning dependent decay (Eq. 4).

CaF [23] in a supersonic jet has recently been reported.

In this paper, we report progress toward an approach to load molecules into a MOT. We combine a two-stage cryogenic He buffer-gas beam source [24] to cool and create an atomic beam and load this directly into a three-dimensional magneto-optical trap (MOT), with no Zeeman slower. We characterize the effects of the buffer-gas background collisions with the trapped atoms and study the feasibility of a three-dimensional MOT for molecules in this manner. The low mean forward velocity of our beam source of ~ 60 m/s renders a Zeeman slower unnecessary for the species studied, and allows for a direct loading of the trap. This shows the way to a simpler experimental path, even in the case of molecules, where it is possible that some slowing will be necessary. In addition, we demonstrate a unique flexibility of this system with regard to the species of choice, since the initial cooling stage relies almost uniquely on collisions with He atoms and not on the internal structure of the species. In particular, we create MOTs of the elements Yb, Tm, Er and Ho, all done in the same setup with no hardware change except tuning the MOT lasers. We load MOTs for the isotopes of mass 170, 171, 172, 174 and 176 of Yb by changing one parameter only, the detuning of the MOT laser frequency.

The total number of atoms in common MOTs for Yb using the 400 nm transition is typically limited to $\sim 4 - 5 \times 10^6$ [25–27] due to spontaneous decay into metastable states during the

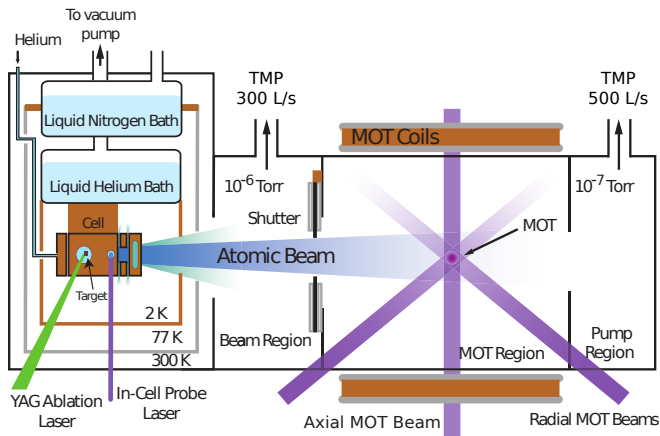


FIG. 2. Schematic of the experimental apparatus. A cryogenic buffer-gas beam source (left) opens into a room-temperature MOT section, separated by a differential pumping region. The photomultiplier tube and imaging system, which are located transversely to the atomic beam, are not depicted. Also not depicted is a 60 L/s turbomolecular pump (TMP) on the MOT region. The distance between the exit of the cell and the MOT is 42 cm.

long loading phases of these traps ($\sim 1 - 10$ s). We can overcome this limitation, given the pulsed nature of our loading scheme, which results in high instantaneous fluxes. Here, in combination with a constant-frequency slowing laser, we further demonstrate that our approach yields a peak number of $4.0(2) \times 10^8$ Yb atoms, which could be potentially important for experiments which desire high MOT numbers.

Although we trap several different elements, we use example species of Ho for our general descriptions. To our knowledge Saffman et al. [28] and this experiment are the first to report laser cooling and trapping of Ho. For background on MOTs for the remaining elements, we refer the reader to the corresponding references: Yb [6], Tm [9] and Er [10, 11].

The lanthanide Holmium has only one stable nuclear isotope, ^{165}Ho . With its nuclear spin quantum number of $I = 7/2$, it has the largest number of hyperfine states of any element, which makes it potentially interesting for qubit implementations [29]. Like other lanthanides, it has a large magnetic dipole moment ($9 \mu_B$). As shown in the level scheme in Fig. 1, the transition at 410.5 nm with a linewidth of $2\pi \times 25$ MHz [30] connecting the $4f^{11}6s^2 (J = 15/2, F = 11)$ and $4f^{11}6s6p (J = 17/2, F = 12)$ states was used for laser cooling. As with previous work on other lanthanides (see e.g. Ref. [9]), no additional repumper was necessary to trap Ho atoms in the MOT, despite the existence of possible decay channels into other hyperfine levels of the ground state manifold.

The apparatus is shown in Fig. 2. A detailed study of the two-stage buffer-gas beam source is described elsewhere [19, 24]. Briefly, the cell, operating at 2.5 K, uses a combination of hydrodynamic extraction and a second slowing stage to produce a cold and effusive-like beam with a peak forward velocity of $\sim 60 - 70$ m/s and FWHM of ~ 70 m/s. A consid-

erable fraction of atoms move below the capture velocity of the atomic MOTs, which is estimated to be $\lesssim 30$ m/s for all species we trap here.

Atoms are introduced into the gas phase by laser ablation of solid precursor targets with 4 ns long pulses with ~ 14 mJ energy from a 532 nm Nd:YAG laser. The atoms thermalize translationally via collisions with the cold He buffer-gas inside the cell to a temperature of around 2 to 4 K and leave the cell to form an atomic beam. He flows between 0.2-4 sccm (standard cubic cm per minute) are used in the experiments. The beam flows from the cryogenic section, through a room temperature beam region, past a shutter, and into the MOT section. The shutter keeps residual He buffer-gas from entering the MOT region when the atomic species of interest is not present. (Atoms are present only for a few ms after the ablation pulse.) For the MOT measurements reported here, the shutter is opened for 10 ms (The shutter lag time is ~ 3 ms.). In order to keep the amount of residual buffer-gas background to a minimum, each section of the chamber is pumped by a turbomolecular pump to maintain a steady-state pressure of $\sim 1 \times 10^{-6}$ Torr in the beam region and $\sim 2 \times 10^{-7}$ Torr in the MOT regions, with the shutter in operation and the buffer-gas flowing in our standard running process.

We detect atoms in the MOT by imaging fluorescence onto a calibrated photomultiplier tube (PMT). For spatial filtering (to cut down background scattering into the PMT), we use an objective that focusses the MOT image through a variable intermediate aperture with a minimal diameter of $\sim 600 \mu\text{m}$. Via simulation of the imaging system using commercial ray-tracing software, we determined the collection efficiency to be $(2.6 \pm 0.5) \times 10^{-3}$.

MOT beams of each species are derived from the same frequency-doubled Ti:Sapphire ring laser. Each MOT beam has ~ 15 mW power with a $1/e^2$ diameter of 9.8 ± 0.5 mm. The Ti:Saph laser is locked to a HeNe laser via a transfer cavity, providing < 5 MHz laser linewidth, which was used to determine the error in the lifetime measurements. The quadrupole field for the MOT is generated from a pair of lab-fabricated water-cooled copper coils, running in an anti-Helmholtz configuration. The coils produced an axial (radial) field gradient of 3.8×10^{-4} T/cm (1.9×10^{-4} T/cm) for the Yb MOT and 1.7×10^{-4} T/cm (0.8×10^{-4} T/cm) for the Tm, Er and Ho MOTs, which was estimated by a finite-element software package.

The loading process of the MOT can be described by a phenomenological differential equation for the number of trapped particles $n(t)$ [31],

$$\frac{dn}{dt} = R(t) - \alpha n(t) - \beta n(t)^2, \quad (1)$$

where $R(t)$ is the loading rate, α the loss due to background gas collisions and β the intra-particle two-body loss. In our measurements, no evidence for two-body effects is observed and, thus, the corresponding term will henceforth be neglected ($\beta = 0$). The loading rate is time-dependent due to the pulsed nature of the loading process. We find that approximating the

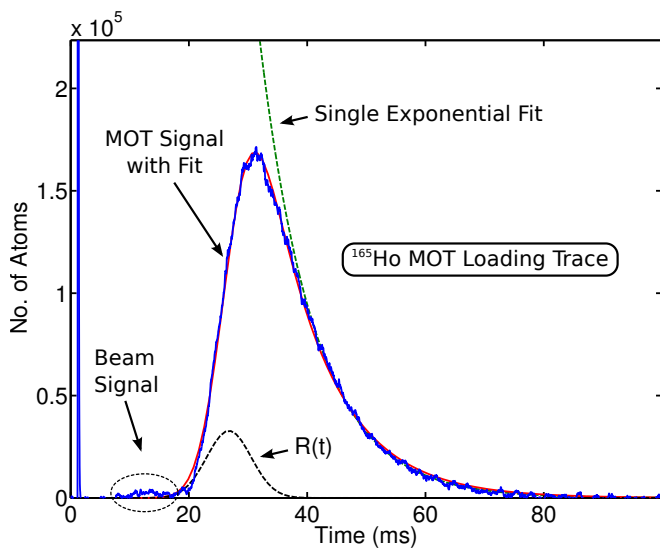


FIG. 3. Time trace of the MOT loading process for Ho with a He flow of 0.3 sccm. The fit to Eq. 3 agrees well with the data and yields the parameters $1/\alpha = 10.1$ ms, $t_0 = 26.8$ ms and $w = 3.76$ ms. Also shown is the corresponding loading rate $R(t)$ to the fit and a single exponential fit for comparison.

loading pulse by a Gaussian function as

$$R(t) = \frac{n_{\text{tot}}}{\sqrt{2\pi}w} \cdot e^{-\frac{(t-t_0)^2}{2w^2}} \quad (2)$$

yields a very good agreement with our measured data. The total number of atoms n_{tot} is defined by the normalization $\int_{-\infty}^{\infty} dt R(t) = n_{\text{tot}}$, where t_0 is the pulse arrival time and w the pulse width. The solution to the loading equation is

$$n(t) = \frac{1}{2} \cdot n_{\text{tot}} \cdot e^{\frac{1}{2}\alpha(-2(t-t_0)+\alpha w^2)} \cdot \left(\text{erf}\left(\frac{t_0 + \alpha w^2}{\sqrt{2}w}\right) - \text{erf}\left(\frac{-t + t_0 + \alpha w^2}{\sqrt{2}w}\right) \right), \quad (3)$$

with the error function defined as $\text{erf}(x) = \frac{2}{\sqrt{\pi}} \int_0^x dt e^{-t^2}$.

An example of a measured time trace of the MOT loading process is shown in Fig. 3 for the case of Ho, along with a fit to the pulsed loading model of Eq. 3. Note that only the tail of the buffer-gas beam signal between 20-30 ms is loaded into the MOT. While the beam signal represents only a velocity class corresponding to a certain detuning, the much larger MOT signal stems from particles from a range of velocities which have been actively cooled and trapped. The resulting peak values for the observed number of atoms loaded into the MOT are given for each element in Table I. Note that the variation among the different species is not only caused by the cooling efficiency given by their corresponding natural linewidths of the cooling transition, but also by the ablation yields, which strongly vary between the specific atoms. The number of trapped atoms can be largely increased by applying low repetition rates of the ablation laser and by using a single-frequency slowing laser. We demonstrate this with one of the elements, namely Yb.

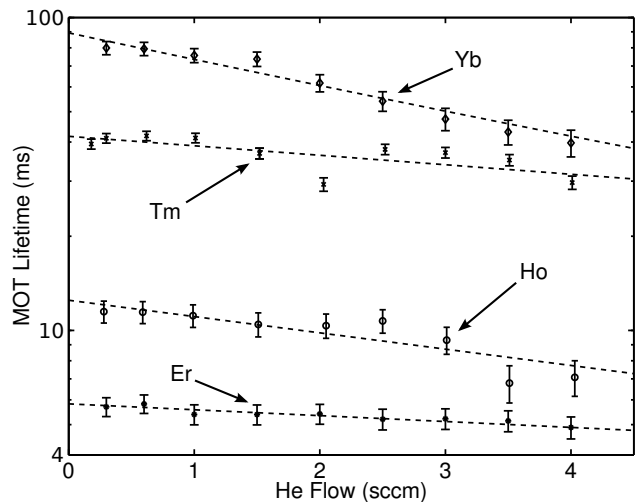


FIG. 4. MOT lifetimes $1/\alpha$ for every species from fitting the time traces to Eq. 3. The dashed lines are exponential fits and act as a guide to the eye only.

Two processes compete with the trap loading and limit the MOT lifetime, namely collisions with the background gas and decay into metastable states. The first process is dominated by residual He buffer-gas in the MOT region. After cold He hits the room-temperature walls of the vacuum chamber, it bounces back and can hit the trapped atoms, leading to losses. In the case of Yb, for example, a head-on collision of an atom at rest with a room-temperature He atom increases its speed by ~ 50 m/s, which means the atom cannot be recaptured into the trap. The measured decrease of MOT lifetimes with varying He flow is shown in Fig. 4. All measurements were taken at the detuning of maximum MOT fluorescence signal. Each point is the result of averaging over five ablation shots. The highest lifetimes for each element were observed for ~ 0.3 sccm He flow and are listed in Table I. The large differences among the species are due to the second lifetime-limiting effect, namely the presence of decay channels to metastable states. Once the atom decays after a

TABLE I. MOT lifetimes, decay rates and peak number of atoms from the fit to Eq. 4 for every species at 0.3 sccm He flow.

	^{174}Yb	^{169}Tm	^{165}Ho	^{166}Er
Γ_0 (s^{-1})	10(2)	21(5)	37(19)	111(17)
Γ_1 (s^{-1})	18(18) ^a	13(24) ^b	895(104)	1307(354) ^c
$1/\alpha$ (ms)	80(4)	41(2)	12(1)	5.7(0.4)
N_{max}	$0.3(2) \times 10^8$	$8(4) \times 10^4$	$1.7(1.0) \times 10^5$	$5(1) \times 10^5$
$N_{\text{max}}^{\text{slow}}$	$4.0(2) \times 10^8$ ^d			

^a Previous work: $23(11) \text{ s}^{-1}$ from Ref. [25].

^b Previous work: $22(6) \text{ s}^{-1}$ from Ref. [9].

^c Previous work: $1695(43) \text{ s}^{-1}$ from Ref. [10].

^d This measurement employs a longitudinal single-frequency slowing laser and a repetition rate of the ablation laser of < 1 Hz.

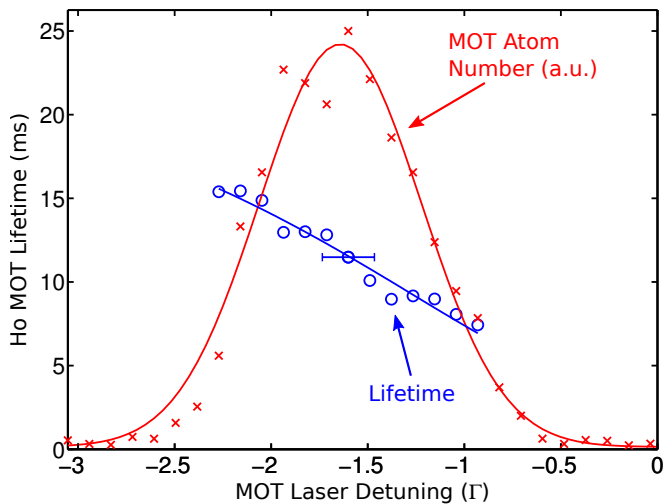


FIG. 5. Ho MOT lifetimes $1/\alpha$ as function of the laser detuning in units of the natural linewidth $\Gamma = 2\pi \times 25$ MHz. Negative values are red-detuned with respect to the line center. The solid line is a fit to Eq. 4 with $\Gamma_0 = 37(19) \text{ s}^{-1}$, $\Gamma_1 = 895(104) \text{ s}^{-1}$. Also shown is the relative atom number in the MOT, including a Gaussian fit as a guide to the eye.

number of photon scattering events into such a dark state, it escapes the cooling and trapping process.

In order to fully describe this decay, for example in the case of Er, 110 intermediate states have to be considered [10]. As a result, theoretical modeling of such complex atoms is rendered to be daunting. Instead, we apply a simplified model [9, 10, 25] which considers a three-level system including trap losses (Fig. 1). In this model, the lifetime $1/\alpha$ scales with the fractional population in the excited state and depends on the laser detuning as

$$\alpha(\Delta) = \Gamma_0 + \Gamma_1 \cdot \left(\frac{s_0/2}{1 + s_0 + 4\Delta^2/\Gamma^2} \right), \quad (4)$$

where Γ_0 represents the loss rate due to background collisions, Γ_1 is the decay rate into intermediate metastable states, s_0 is the saturation parameter, Δ is the laser detuning from the resonance, and $\Gamma = 2\pi \times \Delta\nu$, where $\Delta\nu$ is the natural linewidth. This simplified model omits any population which gets recycled back into the ground state after the decay to the metastable state reservoir, but allows for the determination of a lower limit of the decay rate into the intermediate states.

An example measurement in the case of Ho is shown in Fig. 5. We observe the largest MOT fluorescence signal with a red-detuned laser at approx. -1.6Γ . Although this is the optimal point for high trapped atom numbers, the largest MOT lifetime is observed at detunings further to the red. This effect is explained by the lower population in the excited state and, consequently, a lower probability of decaying into a metastable dark state. On the other hand, increasing the excited state population by moving the laser frequency closer to the transition line center at zero detuning decreases the MOT lifetime almost by a factor of three. The strength of this effect

is governed by the decay rate Γ_1 . The measurement results obtained for each atomic species are summarized in Table I. For the fitting, Γ_0 and Γ_1 were free parameters. The values for Γ_1 for Yb, Tm and Er are in good agreement with previously reported work; for Ho, to our best knowledge, this is the first estimate of the decay rate to metastable states.

In conclusion, we demonstrated the direct loading of magneto-optical traps for Yb, Tm, Er and Ho from a cryogenic He buffer-gas beam source. Despite the presence of the He dominated background gas, we observed lifetimes of up to 80 ms for Yb. Lifetimes of the other species were mainly limited by the decay into metastable dark states and other ground hyperfine states. Additional repumpers can increase the MOT lifetime, as is shown in the case of Tm [9]. We report a decay rate to metastable states for Ho of $895(104) \text{ s}^{-1}$. The great flexibility and low starting temperature of this atomic and molecular source is an ideal precursor for implementing MOTs for species that preclude the common approach of a combination of a high-temperature oven with a Zeeman slower. In particular, recent successful experiments on slowing and cooling diatomic molecules [20–22] reflect this advantage. This, in combination with our work, should demonstrate the feasibility of a light-assisted three-dimensional trap for diatomic molecules using buffer-gas beam sources.

We would like to thank Jun Ye, Mark Yeo, Matthew Hummon, Alejandra Collopy, Benjamin Stuhl and Hsin-I Lu for helpful discussions. We also acknowledge the contributions of Matthew J. Wright to the initial phase of this experiment. This work was supported by the NSF and the ARO.

* boerge@cua.harvard.edu

- [1] J. Helmcke, G. Wilpers, T. Binnewies, C. Degenhardt, U. Sterr, H. Schnatz, and F. Riehle, *IEEE Trans. Instrum. Meas.* **52**, 250 (2003).
- [2] H. Häffner, C. F. Roos, and R. Blatt, *Phys. Rep.* **469**, 155 (2008).
- [3] C. Monroe, *Nature* **416**, 238 (2002).
- [4] J. Weiner, V. S. Bagnato, S. Zilio, and P. S. Julienne, *Rev. Mod. Phys.* **71**, 1 (1999).
- [5] J. R. Anglin and W. Ketterle, *Nature* **416**, 211 (2002).
- [6] K. Honda, Y. Takahashi, T. Kuwamoto, M. Fujimoto, K. Toyoda, K. Ishikawa, and T. Yabuzaki, *Phys. Rev. A* **59**, 934 (1999).
- [7] C. C. Bradley, J. J. McClelland, W. R. Anderson, and R. J. Celotta, *Phys. Rev. A* **61**, 053407 (2000).
- [8] A. Griesmaier, J. Werner, S. Hensler, J. Stuhler, and T. Pfau, *Phys. Rev. Lett.* **94**, 160401 (2005).
- [9] D. Sukachev, A. Sokolov, K. Chebakov, A. Akimov, S. Kanorsky, N. Kholchevsky, and V. Sorokin, *Phys. Rev. A* **82**, 011405 (2010).
- [10] J. J. McClelland and J. L. Hanssen, *Phys. Rev. Lett.* **96**, 143005 (2006).
- [11] A. Frisch, K. Aikawa, M. Mark, A. Rietzler, J. Schindler, E. Zupanič, R. Grimm, and F. Ferlaino, *Phys. Rev. A* **85**, 051401 (2012).
- [12] M. Lu, S. H. Youn, and B. L. Lev,

- Phys. Rev. Lett. **104**, 063001 (2010).
- [13] J. Stuhler, A. Griesmaier, T. Koch, M. Fattori, T. Pfau, S. Giovanazzi, P. Pedri, and L. Santos, Phys. Rev. Lett. **95**, 150406 (2005).
- [14] S. Taie, Y. Rekishu, S. Seiji, and Y. Takahashi, Nature Phys. **8**, 825 (2012).
- [15] P. Rabl, D. DeMille, J. M. Doyle, M. D. Lukin, R. J. Schoelkopf, and P. Zoller, Phys. Rev. Lett. **97**, 033003 (2006).
- [16] D. DeMille, Phys. Rev. Lett. **88**, 067901 (2002).
- [17] L. D. Carr, D. DeMille, R. V. Krems, and J. Ye, New J. Phys. **11**, 055049 (2009).
- [18] R. V. Krems, W. C. Stwalley, and B. Friedrich, *Eds. Cold Molecules: Theory, Experiment, Applications* (CRC Press: Boca Raton, FL, 2009).
- [19] N. R. Hutzler, H.-I. Lu, and J. M. Doyle, Chem. Rev. **112**, 4803 (2012).
- [20] E. S. Shuman, J. F. Barry, and D. DeMille, Nature **467**, 820 (2010).
- [21] J. F. Barry, E. S. Shuman, E. B. Norrgard, and D. DeMille, Phys. Rev. Lett. **108**, 103002 (2012).
- [22] M. T. Hummon, M. Yeo, B. K. Stuhl, A. L. Collopy, Y. Xia, and J. Ye, Phys. Rev. Lett. **110**, 143001 (2013).
- [23] V. Zhelyazkova, A. Cournol, T. E. Wall, A. Matsushima, J. J. Hudson, E. A. Hinds, M. R. Tarbutt, and B. E. Sauer, ArXiv e-prints (2013), arXiv:1308.0421 [physics.atom-ph].
- [24] H.-I. Lu, J. Rasmussen, M. J. Wright, D. Patterson, and J. M. Doyle, Phys. Chem. Chem. Phys. **13**, 18986 (2011).
- [25] T. Loftus, J. R. Bochinski, R. Shivitz, and T. W. Mossberg, Phys. Rev. A **61**, 051401 (2000).
- [26] C. Y. Park and T. H. Yoon, Phys. Rev. A **68**, 055401 (2003).
- [27] Y. Takasu, K. Honda, K. Komori, T. Kuwamoto, M. Kumakura, Y. Takahashi, and T. Yabuzaki, Phys. Rev. Lett. **90**, 023003 (2003).
- [28] J. Miao, J. Hostetter, G. Stratis, and M. Saffman, Bull. Am. Phys. Soc. **58** (2013).
- [29] M. Saffman and K. Mølmer, Phys. Rev. A **78**, 012336 (2008).
- [30] Y. Ralchenko, A. Kramida, J. Reader, and NIST ASD Team, National Institute of Standards and Technology, Gaithersburg, MD (2008).
- [31] A. M. Steane, M. Chowdhury, and C. J. Foot, J. Opt. Soc. Am. B **9**, 2142 (1992).